

This work was written as part of one of the author's official duties as an Employee of the United States Government and is therefore a work of the United States Government. In accordance with 17 U.S.C. 105, no copyright protection is available for such works under U.S. Law.

Public Domain Mark 1.0

<https://creativecommons.org/publicdomain/mark/1.0/>

Access to this work was provided by the University of Maryland, Baltimore County (UMBC) ScholarWorks@UMBC digital repository on the Maryland Shared Open Access (MD-SOAR) platform.

Please provide feedback

Please support the ScholarWorks@UMBC repository by emailing scholarworks-group@umbc.edu and telling us what having access to this work means to you and why it's important to you. Thank you.

RESEARCH LETTER

10.1002/2015GL065856

Key Points:

- HFCs are weak ozone-depleting substances
- HFCs warm the troposphere and stratosphere and modify atmospheric circulation
- In 2050, HFC-125 is projected to be the largest HFC contributor to atmospheric change

Supporting Information:

- Text S1
- Figures S1–S3

Correspondence to:

M. M. Hurwitz,
margaret.m.hurwitz@nasa.gov

Citation:

Hurwitz, M. M., E. L. Fleming,
P. A. Newman, F. Li, E. Mlawer,
K. Cady-Pereira, and R. Bailey (2015),
Ozone depletion by hydrofluorocarbons,
Geophys. Res. Lett., 42, 8686–8692,
doi:10.1002/2015GL065856.

Received 19 AUG 2015

Accepted 30 SEP 2015

Published online 22 OCT 2015

Ozone depletion by hydrofluorocarbons

Margaret M. Hurwitz^{1,2}, Eric L. Fleming^{2,3}, Paul A. Newman², Feng Li^{2,4}, Eli Mlawer⁵,
Karen Cady-Pereira⁵, and Roshelle Bailey^{1,2}
¹Goddard Earth Sciences Technology and Research (GESTAR), Morgan State University, Baltimore, Maryland, USA, ²NASA Goddard Space Flight Center, Greenbelt, Maryland, USA, ³Science Systems and Applications, Inc., Lanham, Maryland, USA, ⁴GESTAR, Universities Space Research Association, Columbia, Maryland, USA, ⁵Atmospheric and Environmental Research, Inc., Lexington, Massachusetts, USA

Abstract Atmospheric concentrations of hydrofluorocarbons (HFCs) are projected to increase considerably in the coming decades. Chemistry climate model simulations forced by current projections show that HFCs will impact the global atmosphere increasingly through 2050. As strong radiative forcers, HFCs increase tropospheric and stratospheric temperatures, thereby enhancing ozone-destroying catalytic cycles and modifying the atmospheric circulation. These changes lead to a weak depletion of stratospheric ozone. Simulations with the NASA Goddard Space Flight Center 2-D model show that HFC-125 is the most important contributor to HFC-related atmospheric change in 2050; its effects are comparable to the combined impacts of HFC-23, HFC-32, HFC-134a, and HFC-143a. Incorporating the interactions between chemistry, radiation, and dynamics, ozone depletion potentials (ODPs) for HFCs range from 0.39×10^{-3} to 30.0×10^{-3} , approximately 100 times larger than previous ODP estimates which were based solely on chemical effects.

1. Introduction

Hydrofluorocarbons (HFCs) are anthropogenic compounds that serve as replacements for both chlorofluorocarbons (CFCs) and hydrochlorofluorocarbons (HCFCs) [United Nations Environment Programme (UNEP), 2012]. In the past three decades, CFCs, HCFCs, halons, and other ozone-depleting substances caused large stratospheric ozone losses, most prominently in the Antarctic (i.e., the so-called “ozone hole”). These compounds contain chlorine (Cl) and/or bromine (Br), and when broken down in the stratosphere, the Cl and Br atoms deplete ozone via catalytic loss cycles. CFCs and HCFCs are regulated by the Montreal Protocol; atmospheric abundances of CFCs are declining while HCFCs are expected to decline in the near future [World Meteorological Organization (WMO), 2014].

HFC concentrations have increased rapidly since 1990 [WMO, 2014]. In the absence of limits on industrial production and the availability of alternatives, atmospheric HFC concentrations are expected to continue to increase through the 21st century [WMO, 2014]. Figure 1 (top) shows time series of the projected surface mixing ratios, from 2000 to 2050, for five HFC species. These five HFCs are, in order of importance, expected to make the largest HFC contributions to global radiative forcing in 2050: HFC-125, HFC-143a, HFC-134a, HFC-32, and HFC-23 (business-as-usual scenario [Miller and Kuijpers, 2011] and high scenario [Velders et al., 2009]). Table 1 lists their atmospheric lifetimes, global warming potentials, and estimated surface radiative forcing. HFC-134a dominated past HFC production [Kim et al., 2011], while HFC-125 is expected to dominate after 2030 [Velders et al., 2009]. HFC-23 is a by-product of HCFC-22 production [Oram et al., 1998]. While HFC-23 emissions have decreased in recent years [Miller et al., 2010], atmospheric concentrations are projected to increase through the mid-21st century, due to the increasing use of HCFC-22 as feedstock in developing countries [Miller and Kuijpers, 2011]. Note that the HFC scenarios shown in Figure 1 and Table 1 present a relative upper bound on projected HFC emissions in 2050 [Gschrey et al., 2011, Figure 3]. HFCs are entirely synthetic and are primarily used in refrigeration and air conditioning, and as foam agents, medical aerosols, fire retardants, and solvents [UNEP, 2012].

While several parties to the Montreal Protocol have recently submitted amendments proposing to control HFCs [e.g., <http://www.state.gov/r/pa/prs/ps/2015/04/240730.htm>], negotiations have progressed slowly in part because of the assertion that “HFCs do not deplete the ozone layer” [UNEP, 2012]. The ozone depletion potential (ODP) of a trace gas species is a relative measure of the change in the global total column ozone per unit mass emission, as compared with that of CFC-11 [Wuebbles, 1983]. ODP calculations incorporate direct,

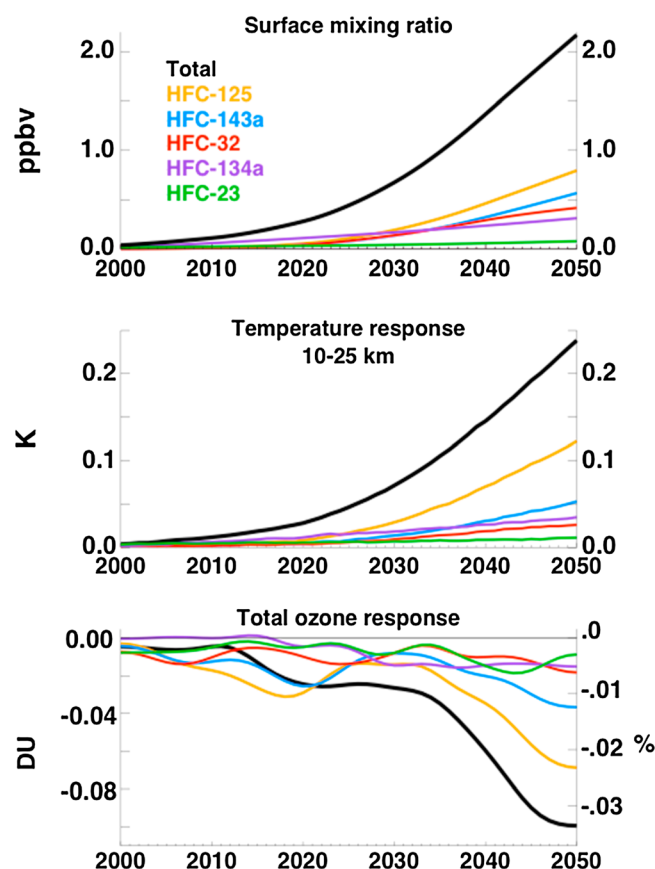


Figure 1. (top) Projected global mean surface mixing ratios for five HFC species (colored lines, ppbv) and their total (black line) from Velders *et al.*'s [2009] high scenario and Miller and Kuijpers' [2011] business-as-usual scenario. (middle) Modeled global mean temperature response (K) in the 10–25 km layer in simulations testing the response to individual HFC species (colored lines) and to all five HFCs simultaneously (black line). (bottom) Same as for Figure 1 (middle) but for the modeled global mean total ozone response (DU, %). The total column ozone time series are smoothed to emphasize the long-term ozone trends.

HFCs made a small contribution to the recent warming of the tropical tropopause [Forster and Joshi, 2005]. Furthermore, HFCs maintain concentrations into the upper stratosphere and mesosphere because of their relatively weak stratospheric loss rates. Of concern to global climate is that HFCs are particularly strong

chemical ozone loss as well as any indirect ozone change, due to a species' ability to modify atmospheric temperature and circulation. The CFCs and halons have the largest ODPs, reflecting their strong chemical reactivity in the stratosphere [WMO, 2014]. In contrast, since HFCs do not contain chlorine or bromine, their estimated direct chemical potential to deplete ozone via catalytic loss cycles that involve fluorine has been shown to be extremely small [Stolarski and Rundel, 1975; Kaye *et al.*, 1991; Ravishankara *et al.*, 1994]. Ravishankara *et al.* [1994] assessed the chemical reactivity of three HFCs and calculated ODPs using a semi-empirical approach combined with a numerical atmospheric chemistry model. Both methods yielded ODPs $< 5 \times 10^{-4}$ (Table 1), leading the authors to conclude that "the ozone depletion potentials related to the presence of the CF_3 group in hydrofluorocarbons are negligibly small." However, no previous HFC assessment has considered their indirect radiative and dynamical impacts on stratospheric ozone.

As atmospheric concentrations of HFCs increase, so will their global climate impact. HFCs absorb infrared radiation in the atmospheric "window" region (8–14 μm) and would be expected to heat the lower atmosphere similarly to other greenhouse gases; fixed dynamical heating calculations determined that

Table 1. Surface Radiative Forcing, 20 and 100 Year Global Warming Potential (GWP), Atmospheric Lifetime, and Simulated Ozone Depletion Potential (ODP) for Five HFC Species

Species	2050 Radiative Forcing (W m^{-2})	20 Year GWP ^c	100 Year GWP ^c	Atmospheric Lifetime (Years) ^d	ODP, This Study and ^c	ODP ^e
HFC-125	0.186 ^a	6,280	3,450	31	$2.9 \pm 0.5 \times 10^{-3}$	3.0×10^{-5}
HFC-143a	0.076 ^a	7,050	5,080	51	$4.2 \pm 1.4 \times 10^{-3}$	
HFC-134a	0.053 ^a	3,810	1,360	14	$1.3 \pm 0.4 \times 10^{-3}$	1.5×10^{-5}
HFC-32	0.045 ^a	2,530	704	5.4	$0.39 \pm 0.18 \times 10^{-3}$	
HFC-23	0.014 ^b	10,800	12,500	228	$30 \pm 6 \times 10^{-3}$	39×10^{-5}
HCFC-22	0.013 ^c	5,310	1,780	12	34×10^{-3c}	
CFC-11	0.035 ^c	7,090	5,160	52	1	

^aVelders *et al.* [2009].

^bMiller and Kuijpers [2011].

^cWMO [2014].

^dSPARC [2013].

^eRavishankara *et al.* [1994], ODP calculations for all altitudes.

radiative forcers: many have large global warming potentials (GWPs), the ratio of their climate impact per unit mass as compared with CO₂, much greater than 1 (Table 1). For example, HFC-125 has a 100 year GWP of 3450; i.e., 1 kg of HFC-125 provides the radiative forcing equivalent to 3450 kg of CO₂ [WMO, 2014]. The radiative forcing by all HFCs is estimated at 19% of the projected CO₂ radiative forcing in 2050 (high scenario [Velders et al., 2009]).

Increasing CO₂ modifies the stratosphere in two ways: First, it accelerates the Brewer-Dobson circulation [Intergovernmental Panel on Climate Change (IPCC), 2013], decreasing ozone in the tropical lower stratosphere and increasing ozone in the extratropics [Li et al., 2009]. Second, increasing CO₂ cools the upper stratosphere, increasing ozone because of the reduction in temperature-dependent ozone loss rates [Haigh and Pyle, 1979]. Using a 3-D chemistry-climate model, Li et al. [2009] found that increasing CO₂ caused a net global increase in total column ozone of 5 Dobson Units (DU) (also known as a “superrecovery” of ozone) by 2060. As for CO₂, taking the radiative and dynamical effects of HFCs into consideration may reveal their potential to modulate ozone. This study represents the first attempt to simulate the atmospheric responses to HFCs directly in a coupled chemistry-climate model. Simulations based on a set of future emission scenarios characterize and estimate the impacts of HFCs on temperature, circulation, and stratospheric ozone in a projected 2050 climate.

2. GSFC 2-D Model and RRTMG IR Parameterization

The Goddard Space Flight Center (GSFC) 2-D (latitude pressure) interactive chemistry, radiation, and dynamics model is described by Fleming et al. [2011], with updates as detailed below. The model domain extends from the ground to approximately 92 km. The model includes a full representation of stratospheric chemistry, including the odd hydrogen, odd nitrogen, radical chlorine and bromine, and methane oxidation cycles. The stratospheric chemistry component computes a full diurnal cycle for 40 fast chemical constituents and has shown to be in good agreement with photochemical steady state box model calculations [Park et al., 1999]. The model gas phase and heterogeneous reaction rates, photochemistry, and lifetimes have been updated according to *Stratospheric Processes and their Role in Climate (SPARC)* [2013].

The GSFC 2-D model is able to simulate various transport-sensitive features in the meridional plane, such as horizontal and vertical gradients of long-lived stratospheric tracers and age-of-air, comparably to observations and to high-performing chemistry-climate models [Fleming et al., 2011; SPARC, 2013]. Also, the GSFC 2-D model simulates long-term changes in stratospheric ozone, temperature, and age of air that are consistent with the three-dimensional Goddard Earth Observing System Chemistry Climate Model (GEOSCCM) in the 1950–2100 period [Fleming et al., 2011].

With the implementation of the Rapid Radiative Transfer Model for General Circulation Model Applications (RRTMG) IR parameterization (see supporting information) in the GSFC 2-D model, and the explicit addition of six fluorinated species, predicted distributions of water vapor, ozone, the primary greenhouse gases (CO₂, CH₄, and N₂O), CFC-11, CFC-12, and HCFC-22, five HFC species (HFC-23, HFC-32, HFC-125, HFC-134a and HFC-143a), and CF₄ feed back to the radiative calculations. The major loss processes for HFCs are reactions with OH, especially in the tropical troposphere; since the model does not include interactive tropospheric chemistry, tropospheric OH is specified from a seasonal climatology [Spivakovsky et al., 2000].

The atmospheric impacts of HFCs are simulated in the GSFC 2-D model by varying the emissions of five HFC species. These species are projected to make the largest HFC contributions to global surface radiative forcing in 2050: HFC-125, HFC-143a, HFC-134a, HFC-32, and HFC-23 (Table 1). The surface radiative forcing of an HFC species is the product of the predicted surface mixing ratio [Miller and Kuijpers, 2011; Velders et al., 2009] and that species' radiative efficiency [IPCC, 2013]. In 2050, the sum of the surface radiative forcing perturbations by the above five HFC species is 0.38 W m⁻²; the total surface mixing ratio perturbation is approximately 2 ppbv. Simulations were initialized in 2000 and run through 2050 with flux-based boundary conditions representing potential future emissions of four HFCs (HFC-32, HFC-125, HFC-134a, and HFC-143a; high scenario [Velders et al., 2009]) surface mixing ratio boundary conditions were imposed for HFC-23 (business-as-usual scenario [Miller and Kuijpers, 2011]). In addition to a simulation with zero HFC emissions, six additional simulations tested the atmospheric response to imposing the five HFC emissions scenarios simultaneously and to imposing the scenario for each individual HFC species. In all simulations, surface mixing ratio boundary conditions were imposed for CO₂, CH₄, N₂O (Representative Concentration Pathways 6.0 scenario [Fujino et al., 2006])

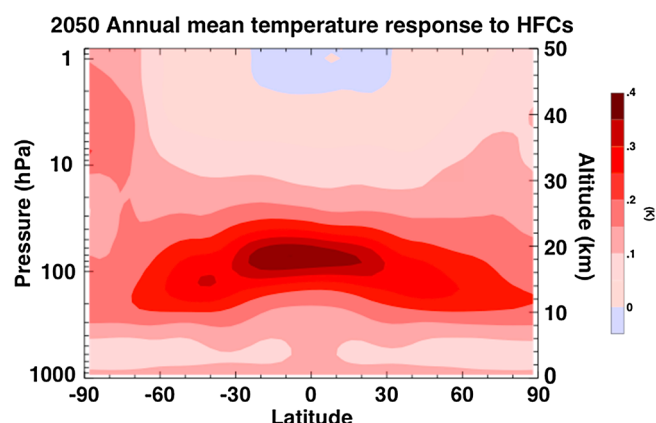


Figure 2. Annual mean temperature response (K) to HFCs in a 2050 climate.

et al., 2011]. As in *Fleming et al.* [2011], a latitudinally dependent long-term trend derived from GEOSCCM simulations accounts for future CO_2 -induced increases in surface temperature. For the HFC simulations, the global mean surface temperature response to changes in HCFC-22 [Kratz *et al.*, 1993] is scaled by the radiative efficiency of each HFC species. HCFC-22 was chosen as the reference gas for this purpose, since the IR-driven temperature response distribution to an HCFC-22 perturbation is similar to that of the HFCs. The global mean surface temperature perturbation in the simulation with all HFCs is 0.13 K in 2050. Sensitivity simulations, either doubling the magnitude of the surface forcing or running the model with zero surface forcing, show that the HFC-related temperature response is most sensitive to the surface forcing in the lower troposphere, i.e., at the model levels closest to the model's lower boundary. The temperature response above 10 km is relatively insensitive to the imposed surface temperature forcing, varying by 10–20% in response to the doubling or removal of the surface forcing.

3. Results

HFCs warm the troposphere and stratosphere. Figure 2 shows the difference in the 2050 annual mean temperature in the simulation that includes HFCs as compared with the simulation without HFCs. The warming response to HFCs increases with height from the troposphere into the lower stratosphere, with the maximum of 0.41 K seen at 8°S, 72 hPa, and decreases with height in the middle stratosphere. Near-zero temperature response is reached in the uppermost stratosphere and mesosphere. The vertical profile of the temperature response to HFC-134a is similar to that estimated by *Forster and Joshi* [2005]. Note that because of differences in their IR absorption spectra, the structure of the heating response to HFCs closely resembles that of the CFCs (i.e., with maximum heating ~18 km altitude) but is different from that of CO_2 (with tropospheric warming and stratospheric cooling) [Forster and Joshi, 2005; Li *et al.*, 2009]. Figure 1 (middle) shows time series of the global mean temperature response between 10 and 25 km for the five HFCs individually and as a group. HFC-125 makes the largest contribution to the warming of the upper troposphere and stratosphere, accounting for approximately half (0.11 K) of the annual mean warming (0.23 K) in 2050.

A 0.4 K warming of the tropical tropopause by HFCs would be expected to increase tropical lower stratospheric water vapor by approximately 0.25 ppmv [Oman *et al.*, 2008]. A sensitivity simulation shows that an imposed increase in water vapor entering the stratosphere leads to additional net depletion of global total column ozone. Therefore, including the water vapor would further increase the impact of HFC-forced ozone depletion. However, proper quantification of this water feedback effect requires a fully coupled, 3-D ocean atmosphere chemistry model that captures the complex radiative feedbacks between temperatures, clouds, and water vapor.

The stratospheric meridional overturning (or Brewer-Dobson) circulation is characterized by upward motion (positive w^* , the vertical component of this overturning circulation) in the tropics and by downward motion (negative w^*) at high latitudes (Figure 3). Above 18 km, HFCs enhance this circulation. In Figure 3, streamlines show the HFC-related enhancement of the upward motion in the tropical stratosphere and the enhanced downward motion poleward of 40° latitude. The structure of the HFC-related w^* changes mimics that found for enhanced CO_2 , but the magnitude of the changes is smaller [Li *et al.*, 2009]. The mean age of air,

and for the ozone-depleting substances (A1 scenario [WMO, 2014]). In this study, the results labeled as the “2050 annual mean response” represent the average response for model years 2049 and 2050.

As the GSFC 2-D model is an atmosphere-only model, boundary conditions must be specified at the surface. At the start of each simulation, the latitude and seasonal surface temperature distributions are based on the 1994–2014 average of the Modern Era Reanalysis for Research and Applications reanalysis [Rienecker

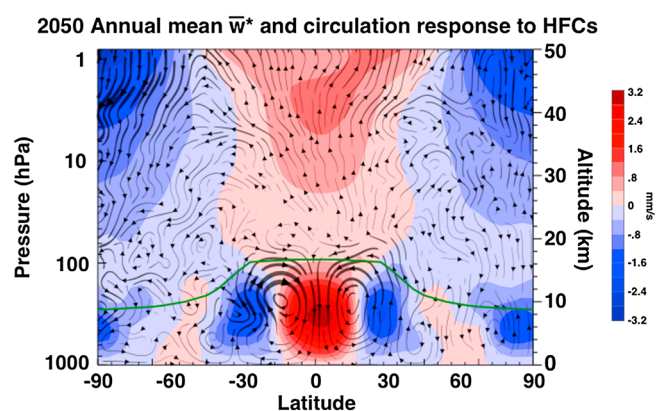


Figure 3. Annual mean residual circulation response (streamlines) to HFCs in a 2050 climate. Colored contours show the annual mean vertical velocity (w^* ; mm s^{-1}); red contours indicate ascending motion while blue contours indicate descent. The magnitude of the HFC-related change in circulation is approximately 1% that of the baseline simulation in 2050. The green line indicates the mean position of the tropopause.

–0.035% (–0.10 DU) in 2050. The ozone response to HFCs results from temperature and circulation changes; sensitivity simulations show that 35% of the global mean total ozone change is driven by temperature changes (i.e., temperature impacts on gas phase and heterogeneous reactions), while the remainder is driven by circulation changes. The HFC-related ozone response is weak as compared with the 2.5% ozone depletion by CFCs and other chlorine- and bromine-containing species [WMO, 2014] in the 1980s and 1990s in the 60°S–60°N region.

Figure 4 shows the latitudinal and vertical structure of the annual mean ozone response to HFCs in 2050. The largest ozone responses are in the tropical upper troposphere/lower stratosphere, the Antarctic lower stratosphere, and in the middle stratosphere. Additional simulations that isolate the contributions of the temperature-dependent gas phase and/or heterogeneous chemistry are used to attribute the causes of the response (not shown). These additional simulations reveal that the negative ozone response is due partly to higher temperatures (Figure 2), which enhance the temperature-sensitive Chapman and odd hydrogen catalytic ozone loss cycles. This response to increasing HFCs has the opposite sign as that of CO_2 ; *Li et al.* [2009] found an upper stratospheric cooling and thus a net increase in total ozone. Also, at tropical to mid-latitudes, the negative ozone response results from enhanced upwelling (or weakened downwelling) (Figure 3). Since ozone concentrations increase sharply with height in this region, the circulation response to HFCs enhances the advection of ozone-poor air from below (in regions of mean ascent) and weakens the advection of ozone-rich air from above (in regions of mean descent).

A positive ozone response occurs in the tropical stratosphere, below 20 km, where a slower ascent rate (Figure 3) allows for greater photochemical production of ozone in an air parcel [Avalone and Prather, 1996].

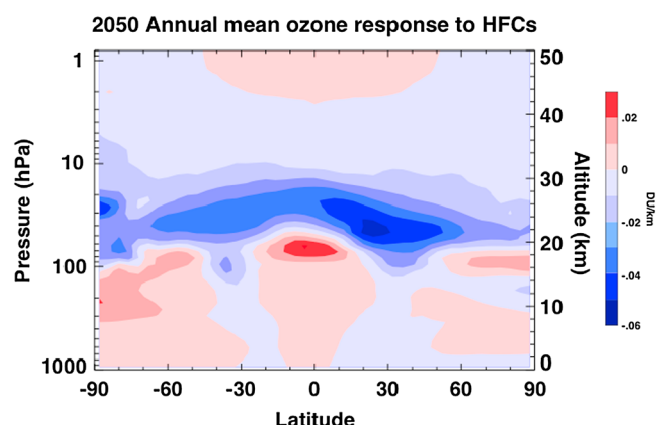


Figure 4. Annual mean ozone response (DU km^{-1}) to HFCs in a 2050 climate.

a passive tracer measuring the time since air has passed through the tropical tropopause region, decreases slightly throughout the stratosphere (by –0.3% or –0.015 years; not shown), reflecting the enhancement of the Brewer-Dobson circulation. Below 18 km, in the tropics and subtropics, the HFC-induced changes oppose the direction of the mean circulation (i.e., weakening of the Hadley circulation).

Integrated over the atmospheric column, the global mean ozone response is negative, that is, HFC emissions lead to a net stratospheric ozone loss. Figure 1 (thick black line, bottom) shows that the total column ozone response to HFCs is approximately

Small, positive ozone responses occur in the polar regions below ~20 km. In the polar lower stratosphere, warming (Figure 2) reduces heterogeneous polar ozone loss. This effect slightly outweighs ozone reductions caused by both enhanced gas phase loss cycles and changes in the circulation (Figure 3). Thus, HFCs would be expected to make a positive but very weak net effect on Antarctic ozone recovery.

The contributions of the five HFC species to warming in the 10–25 km layer, and to the total column ozone loss, are shown in Figure 1 (middle and

bottom, respectively). HFC-125 makes the largest contribution of approximately half of the net temperature and total ozone responses in 2050.

The stratosphere responds linearly to changing HFC concentrations: the response to the simulation that incorporates all five HFCs is nearly equal to the sum of the individual responses to HFCs. Figure S2 in the supporting information shows that the magnitude of the surface radiative forcing by each HFC species is strongly correlated with its atmospheric temperature and total column ozone responses. Further, the relationship between the surface radiative forcing and the simulated HFC responses does not depend on the HFC emission scenario: The temperature and total ozone responses to HFC-125 are smaller in *Velders et al.*'s [2009] low scenario (Figure S2, yellow shapes with red outlines) than in *Velders et al.*'s [2009] high scenario (yellow shapes with black outlines), reflecting the proportionally smaller surface radiative forcing (Figure S2) and lower projected surface mixing ratios (Figure S3).

ODPs are based on individual, 30 year, steady state simulations for each HFC species, with 2050 climate conditions but with a perturbation of the surface mixing ratio equal to that species' projected change between 2000 and 2050. In an additional simulation, CFC-11 is perturbed by 1 ppbv to obtain a reduction in global total ozone of approximately 0.01%, similar to the perturbation made by HFCs. The resulting ODP value represents the change in global total column ozone per unit mass emission of an individual HFC species, relative to that of CFC-11, averaged over the final 10 years of each simulation. The 2050 estimates of ODPs for HFCs range from 0.39×10^{-3} to 30.0×10^{-3} (Table 1). These values are approximately 100 times larger than the direct, chemical ODPs for HFC-23, HFC-134a, and HFC-125 as calculated by *Ravishankara et al.* [1994] (Table 1). Also, note that the new ODP value for HFC-23 is comparable with an estimate of the direct, chemical ODP for HCFC-22 [WMO, 2014] (Table 1), as well as an ODP estimate for N₂O which considered both its direct and indirect ozone impacts [Fleming et al., 2011].

Although the simulated ozone responses to HFCs are strongly correlated with surface radiative forcing (Figure S2), differences from a perfect linear fit affect the ODP estimates. The range of ODP estimates for an HFC species stems from the competing processes that impact the ozone response (both positively and negatively, as discussed above), interannual stratospheric variability, and ozone responses that are small as compared with the background climate variability. Note that the range of ODPs for the, e.g., CFCs would be expected to be smaller than that for the HFCs, since for the CFCs, direct chemical ozone loss dominates over other processes. The ODP error estimates provided in Table 1 represent differences between ODP calculations based on *Velders et al.*'s [2009] high and low scenarios (HFC-32, HFC-125, HFC-134a, and HFC-143a) and between *Miller and Kuijpers*' [2011] business-as-usual and best practices scenarios (HFC-23).

4. Conclusions and Discussion

Numerical chemistry-climate model simulations show that, in a projected 2050 climate, HFCs modify atmospheric temperature and circulation, leading to stratospheric ozone depletion. HFCs warm the troposphere and stratosphere, with a peak tropical warming of 0.41 K at 72 hPa and a global average warming of 0.23 K in the 10–25 km layer. The global mean, total column ozone net depletion is small (0.10 DU), reflecting the near cancellation of the gas phase response (negative), heterogeneous ozone loss (positive), and changes in circulation (both negative and positive). HFC-125 accounts for approximately half of the simulated changes in temperature and ozone in 2050. In the GSFC 2-D model, 2050 ODPs for HFCs range from 3.9×10^{-4} to 3.0×10^{-2} . HFCs have nonzero ODPs and thus are weak ozone-depleting substances.

This study considered simulations based on one scenario for future HFC emissions [Miller and Kuijpers, 2011; Velders et al., 2009]. However, recent U.S. and European Union restrictions on HFC production and usage may restrict global emissions of these HFC species in the coming years (see http://ec.europa.eu/clima/policies/ff-gas/legislation/index_en.htm; http://www.epa.gov/ozone/snap/download/SAN_5750_SNAP_Status_Change_Rule_FINAL_RULE_signature_version-signed-7-2-2015.pdf) and in turn lessen the atmospheric impacts of HFCs by 2050. However, this study found the impacts of HFCs to be generally linear and scalable (i.e., the simulated responses to HFC-125 in *Velders et al.*'s [2009] high and low scenarios; see Figure S2). Hence, if HFC emissions were reduced by 50%, the stratospheric impacts on ozone, temperature, and circulation would be reduced by a comparable amount.

Likewise, the integrated effects of all HFCs may be somewhat larger than those presented above. This study considered only the five HFC species expected to make the largest contributions to future HFC-related changes in climate and ozone. The results of this study suggest that HFC-152a, HFC-245fa, HFC-365mfc [Velders *et al.*, 2009], and other emerging HFC species that make small contributions to surface radiative forcing would have temperature and ozone impacts qualitatively similar to those of, e.g., HFC-125, but with proportionately smaller magnitudes. For example, if accounting for additional HFC species were to increase the surface radiative forcing by 0.05 W m^{-2} (to a total of 0.43 W m^{-2} in 2050), the results of this study suggest that the resulting temperature response in the 10–25 km layer would be $\sim 0.26 \text{ K}$ with an $\sim 0.11 \text{ DU}$ net reduction in total column ozone.

Acknowledgments

The authors thank A. Douglass, C. Jackman, Q. Liang, R. Stolarski, and two anonymous reviewers for their helpful suggestions. The authors acknowledge funding from the NASA ACPMAP program. The NASA GSFC 2-D model output will be made available upon request.

References

- Avallone, L. M., and M. J. Prather (1996), Photochemical evolution of ozone in the lower tropical stratosphere, *J. Geophys. Res.*, **101**(D1), 1457–1461, doi:10.1029/95JD03010.
- Fleming, E. L., C. H. Jackman, R. S. Stolarski, and A. R. Douglass (2011), A model study of the impact of source gas changes on the stratosphere for 1850–2100, *Atmos. Chem. Phys.*, **11**, 8515–8541, doi:10.5194/acp-11-8515-2011.
- Forster, P. M. D., and M. Joshi (2005), The role of halocarbons in the climate change of the troposphere and stratosphere, *Clim. Change*, **71**, 249–266, doi:10.1007/s10584-005-5955-7.
- Fujino, J., R. Nair, M. Kainuma, T. Masui, and Y. Matsuoka (2006), Multigas mitigation analysis on stabilization scenarios using AIM global model, multigas mitigation and climate policy, *Energ. J. Spec. Issue*, **27**, 343–353.
- Gschrey, B., W. Schwarz, C. Elsner, and R. Engelhardt (2011), High increase of global F-gas emissions until 2050, *Greenhouse Gas Meas. Manage.*, **1**, 85–92, doi:10.1080/20430779.2011.579352.
- Haigh, J. D., and J. A. Pyle (1979), A two-dimensional calculation including atmospheric carbon dioxide and stratospheric ozone, *Nature*, **279**, 222–224.
- Intergovernmental Panel on Climate Change (IPCC) (2013), *Climate Change 2013: The Physical Science Basis, Contribution of Working Group I to the Fifth Assessment Report of the Intergovernmental Panel on Climate Change*, edited by T. F. Stocker *et al.*, 1535 pp., Cambridge Univ. Press, Cambridge, U. K., and New York.
- Kaye, J. A., A. R. Douglass, C. H. Jackman, and R. S. Stolarski (1991), Two-dimensional model calculation of fluorine-containing reservoir species in the stratosphere, *J. Geophys. Res.*, **96**, 12,865–12,881, doi:10.1029/91JD01178.
- Kim, K.-H., Z.-H. Shon, H. T. Nguyen, and E.-C. Jeon (2011), A review of major chlorofluorocarbons and their halocarbon alternatives in the air, *Atmos. Environ.*, **45**, 1369–1382, doi:10.1016/j.atmosenv.2010.12.029.
- Kratz, D. P., M.-D. Chou, and M. M.-H. Yan (1993), Infrared radiation parameterizations for the minor CO₂ bands and for several CFC bands in the window region, *J. Clim.*, **6**, 1269–1281.
- Li, F., R. S. Stolarski, and P. A. Newman (2009), Stratospheric ozone in the post-CFC era, *Atmos. Chem. Phys.*, **9**, 2207–2213.
- Miller, B. R., and L. J. M. Kuijpers (2011), Projecting future HFC-23 emissions, *Atmos. Chem. Phys.*, **11**, 13,259–13,267, doi:10.5194/acp-11-13259-2011.
- Miller, B. R., *et al.* (2010), HFC-23 (CHF₃) emission trend response to HCFC-22 (CHClF₂) production and recent HFC-23 emission abatement measures, *Atmos. Chem. Phys.*, **10**, 7875–7890, doi:10.5194/acp-10-7875-2010.
- Oman, L. D., D. W. Waugh, S. Pawson, R. S. Stolarski, and J. E. Nielsen (2008), Understanding the changes of stratospheric water vapor in coupled chemistry-climate model simulations, *J. Atmos. Sci.*, **65**, 3278–3291, doi:10.1175/2008JAS2696.1.
- Oram, D. E., W. T. Sturges, S. A. Penkett, A. McCulloch, and P. J. Fraser (1998), Growth of fluorofom (CHF₃, HFC-23) in the background atmosphere, *Geophys. Res. Lett.*, **25**, 35–38, doi:10.1029/97GL03483.
- Park, J. H., *et al.* (1999), Models and Measurements Intercomparison II, NASA Tech. Memo. NASA/TM-1999-209554.
- Ravishankara, A. R., *et al.* (1994), Do Hydrofluorocarbons Destroy Stratospheric Ozone?, *Science*, **263**, 71–75, doi:10.1126/science.263.5143.71.
- Rienecker, M. M., *et al.* (2011), MERRA: NASA's Modern-Era Retrospective Analysis for Research and Applications, *J. Clim.*, **24**, 3624–3648.
- Stratosphere-Troposphere Processes and their Role in Climate (SPARC) (2013), *Lifetimes of Stratospheric Ozone-Depleting Substances, Their Replacements, and Related Species – Rep. 6*, edited by M. K. W. Ko *et al.*
- Spivakovsky, C. M., *et al.* (2000), Three-dimensional climatological distribution of tropospheric OH: Update and evaluation, *J. Geophys. Res.*, **105**(D7), 8931–8980, doi:10.1029/1999JD901006.
- Stolarski, R. S., and R. D. Rundel (1975), Fluorine photochemistry in the stratosphere, *Geophys. Res. Lett.*, **2**, 443–444.
- United Nations Environment Programme (UNEP) (2012), HFCs: A critical link in protecting climate and the ozone layer, UNEP, 36 pp. [Available at http://www.unep.org/dewa/Portals/67/pdf/HFC_report.pdf.]
- Velders, G. J. M., D. W. Fahey, J. S. Daniel, M. McFarland, and S. O. Andersen (2009), The large contribution of projected HFC emissions to future climate forcing, *Proc. Natl. Acad. Sci. U.S.A.*, **106**(27), 10,949–10,954.
- World Meteorological Organization (WMO) (2014), Scientific Assessment of Ozone Depletion: 2014, Global Ozone Research and Monitoring Project – Rep. 55, Geneva, Switzerland.
- Wuebbles, D. J. (1983), Chlorocarbon emission scenarios: Potential impact on stratospheric ozone, *J. Geophys. Res.*, **88**(C2), 1433–1443, doi:10.1029/JC088iC02p01433.